

# Redshift distortions in one-dimensional power spectra

Vincent Desjacques and Adi Nusser

*The Physics Department and the Asher Space Research Institute, Technion, Haifa 32000, Israel*  
*Email : dvince@physics.technion.ac.il, adi@physics.technion.ac.il*

30 November 2018

## ABSTRACT

We present a model for one-dimensional (1D) matter power spectra in redshift space as estimated from data provided along individual lines of sight. We derive analytic expressions for these power spectra in the linear and nonlinear regimes, focusing on redshift distortions arising from peculiar velocities. In the linear regime, redshift distortions enhance the 1D power spectra only on small scales and do not affect the power on large scales. This is in contrast to the effect of distortions on three-dimensional (3D) power spectra estimated from data in 3D space, where the enhancement is independent of scale. For CDM cosmologies the 1D power spectra in redshift and real space are similar for wavenumbers  $q \lesssim 0.1 \text{ hMpc}^{-1}$  where both have a spectral index close to unity, independent of the details of the 3D power spectrum. Nonlinear corrections drive the 1D power spectrum in redshift space into a nearly universal shape over scales  $q \lesssim 10 \text{ hMpc}^{-1}$ , and suppress the power on small scales as a result of the strong velocity shear and random motions. The redshift space 1D power spectrum is mostly sensitive to the amplitude of the initial density perturbations. Our results are useful in particular for power spectra computed from the SDSS quasars sample.

## Key words:

intergalactic medium - quasars: absorption lines - cosmology: theory – gravitation – dark matter

## 1 INTRODUCTION

Measurement of distances in cosmology is only possible for nearby cosmic objects, and even there it is plagued with observational biases. Velocities, however, are directly measured by means of the Doppler redshifts. Most observational data is therefore described in terms of redshifts. Three dimensional galaxy surveys provide the angular positions and the redshifts of galaxies. Absorption lines in quasars (QSO) spectra are characterized by their redshift coordinate along lines of sight (LOS) to quasars. Redshifts differ from distances by the peculiar velocities (deviations from pure Hubble flow) along the line of sight. This causes systematic differences between the spatial distribution of data in redshift and distance space. These differences are termed redshift distortions. On large scales, these redshift distortions amount to an enhancement of the power spectrum estimated from the galaxy distributions in redshift surveys. In a seminal paper, Kaiser (Kaiser 1987, see also Lilje & Efstathiou 1989, McGill *et al.* 1990) derived an expression which accounts for the effect of linear peculiar motions in three-dimensional (3D) power spectra. Since then, the impact of redshift distortions on the 3D power spectrum (and higher order statistics) has been studied intensively using analytic and numerical

methods to constrain  $\Omega_\Lambda$  and  $\Omega_m$  from measurements of the distortions parameter  $\beta$  (e.g. Peacock 1992; Hamilton 1993; Peacock & Dodds 1994; Fisher, Sharf & Lahav 1994; Cole, Fisher & Weinberg 1994; Fisher & Nusser 1996; Ballinger, Peacock & Heavens 1996; Loveday *et al.* 1996; Ratcliffe *et al.* 1996; Taylor & Hamilton 1996; Heavens & Matarrese & Verde 1998; Magira, Jing & Suto 2000; Kang *et al.* 2002)

In this paper we will focus on the effect of redshift distortions in one-dimensional (1D) power spectra, as they could be computed from data along individual lines of sight. We will also address how nonlinear corrections affect the shape and the amplitude of the 1D redshift space power spectrum. To model the linear and nonlinear evolution of 1D power spectra, we will rely on analytic formulae which have been calibrated by means of numerical simulations (e.g. Bardeen *et al.* 1986; Smith *et al.* 2003). The subject of this work is timely in view of the large sample of QSOs now provided by the Sloan Digital Sky Survey (SDSS). The SDSS collaboration obtained spectra of comoving length  $\sim 80 \text{ h}^{-1}\text{Mpc}$  for  $\sim 100000$  quasars, with spectral resolution  $R \sim 2000$  in the range 3800-9200Å (e.g. Abazajian *et al.* 2003). These spectra will improve significantly the statistics of the (dimensionless) flux power spectrum  $\Delta_F$  of the

Ly $\alpha$  forest which has been extensively used in the past years to constrain the linear 3D matter power spectrum  $\Delta_{3D}^s$  (e.g. Croft *et al.* 1998, 1999, 2002; McDonald *et al.* 2000, McDonald 2003).

The paper is organized as follow. In §2 we present our notation and briefly review the linear theory of redshift distortions in 3D power spectra. In §3 we apply linear theory to model distortions in 1D power spectra. In §4 we extend the analysis to include nonlinear effects. We conclude with a discussion of our results in §5.

## 2 BASIC RELATIONS

In this section we describe briefly the basic definitions and relations relevant to our calculations of redshift distortions in 1D power spectra.

Our notation is as follows. The comoving real space (distance) and redshift coordinates, both in  $\text{km s}^{-1}$ , are denoted by  $\mathbf{x}$  and  $\mathbf{s}$ , respectively. The comoving peculiar velocity in  $\text{km s}^{-1}$  at position  $\mathbf{x}$  is  $\mathbf{v}$ . The local density of a distribution of particles is  $\rho$  and the corresponding density contrast is  $\delta = \rho/\bar{\rho} - 1$  where  $\bar{\rho}$  is the mean density. The cosmological mass density and vacuum energy parameters are  $\Omega_m$  and  $\Omega_\Lambda$  respectively. The superscripts  $r$  and  $s$  will designate quantities in real and redshift space, respectively.

### 2.1 3D and 1D power spectra

The three-dimensional Fourier transform of a 3D field  $f(\mathbf{x})$  is

$$f_{\mathbf{k}}^{3D} = \int \frac{d^3\mathbf{x}}{(2\pi)^3} \exp(-i\mathbf{k}\cdot\mathbf{x}) f(\mathbf{x}). \quad (1)$$

If the field  $f$  is given only along the  $z$  axis, we then define its 1D Fourier transform at a wavenumber  $q$  as

$$f_q^{1D} = \int \frac{dz}{2\pi} \exp(-iqz) f(z), \quad (2)$$

where for brevity we denote a point on the  $z$  axis only by its  $z$  coordinate (the  $x$  and  $y$  coordinates being zeros). We can express  $f_q^{1D}$  in terms of  $f_{\mathbf{k}}^{3D}$  as (e.g. Kaiser & Peacock 1991)

$$f_q^{1D} = \int \frac{d^2\mathbf{k}_\perp}{(2\pi)^2} f_{\mathbf{k}_\parallel=q, \mathbf{k}_\perp}^{3D}, \quad (3)$$

where  $k_\parallel$  and  $\mathbf{k}_\perp$  are the components of  $\mathbf{k}$  parallel and perpendicular to the  $z$  axis. It should be noted that this relation holds in real and redshift space.

Using (3) the covariance matrices of the 1D and 3D Fourier modes are given by

$$\langle f_{q'}^s f_q^s \rangle = \int \frac{d^2\mathbf{k}_\perp}{(2\pi)^2} \int \frac{d^2\mathbf{k}_\perp'}{(2\pi)^2} \langle f_{q', \mathbf{k}_\perp'}^{3Ds} f_{q, \mathbf{k}_\perp}^{3Ds} \rangle. \quad (4)$$

The 3D and 1D power spectra are given in terms of the covariance matrices by  $\langle f_{\mathbf{k}}^{3D} f_{\mathbf{k}'}^{3D} \rangle = (2\pi)^3 P_{3D}(\mathbf{k}) \delta_D(\mathbf{k} + \mathbf{k}')$ , and  $\langle f_q f_{q'} \rangle = 2\pi P_{1D}(q) \delta_D(q + q')$ . We work with the dimensionless power spectrum  $\Delta$ , which is the density variance per logarithmic interval of wavenumber  $k$ . Adopting the convention of Peebles (1980), we have

$$\Delta_{3D}(k) = \frac{k^3}{2\pi^2} P_{3D}(k), \quad \Delta_{1D}(k) = \frac{k}{\pi} P_{1D}(k). \quad (5)$$

Using (3) and (4) we arrive at the relation

$$\Delta_{1D}(q) = \frac{q}{2\pi} \int d^2\mathbf{k}_\perp \frac{\Delta_{3D}(q, \mathbf{k}_\perp)}{(q^2 + \mathbf{k}_\perp^2)^{3/2}}. \quad (6)$$

This a general relation which is valid for 3D and 1D power spectra in real and redshift space. This relation will be the basis of our calculation of redshift distortions in 1D power spectra.

### 2.2 Redshift distortions

The corresponding redshift space coordinate, also in  $\text{km s}^{-1}$ , is

$$\mathbf{s} = \mathbf{x} + v_\parallel(\mathbf{x}), \quad (7)$$

where  $v_\parallel(\mathbf{r}) = \mathbf{v} \cdot \hat{\mathbf{x}}$ , and  $\hat{\mathbf{x}} = \mathbf{x}/|\mathbf{x}|$  is the unit vector along the line of sight. Assuming a one-to-one mapping between  $\mathbf{x}$  and  $\mathbf{s}$ , the density in redshift space,  $\rho^s$ , can be related to  $\rho^r$  by means of the equation of mass conservation (continuity)

$$\rho^s(\mathbf{s}) d^3\mathbf{s} = \rho^r(\mathbf{x}) d^3\mathbf{x}. \quad (8)$$

Using (7) and expanding the continuity equation to first order in  $\delta^{s,r}$  and  $dv_\parallel/dr$  yields

$$\delta^s(\mathbf{s}) = \delta^r(\mathbf{x}) - \frac{dv_\parallel}{dr}(\mathbf{x}), \quad (9)$$

The continuity equation (8) and its linearised version (9) refer to the distribution of any points that have the velocity field  $v_\parallel$ . In this paper we are mainly interested in the effect of redshift distortions in 1D matter power spectra, and the fluctuation field  $\delta^r$  is simply the matter density contrast  $\delta_m^r$ . The present calculation can be extended to fluctuation fields which are closely related to the underlying mass (dark matter) distribution by means of a linear bias factor,  $b$  (e.g. Kaiser 1987). In this case,  $\delta^r = b\delta_m^r$  where  $\delta_m^r$  is the real space mass density contrast. In the case of galaxy surveys,  $b$  is the traditional bias factor between the galaxy and mass distributions.

### 2.3 Linear distortions in 3D power spectra

As clear from equation (9), a quantification of the effect of redshift distortions on the properties of an observed field  $\delta^s$  requires knowledge of the velocity field  $\mathbf{v}$ . Over scales where the density contrast is small, linear theory yields the relation

$$\delta^r = -\beta^{-1} \nabla \cdot \mathbf{v}, \quad (10)$$

where  $\beta$  is proportional to the logarithmic derivative of the growth factor,  $\text{dln}D_+/\text{dln}a$  (e.g. Peebles 1980).  $\beta \approx \Omega_m(z)^{0.6}/b$  is a good approximation for a wide range of CDM models. Hence, at redshift  $z \gtrsim 1$ , one can safely assume  $\beta \approx b^{-1}$ .

In linear theory, the 3D power spectra of  $\delta^s$  and  $\delta^r$  can be related as follows (e.g. Kaiser 1987). Assuming potential flow, i.e. that the velocity is derived from a potential, the linear theory relation can be expressed in Fourier space as

$$\mathbf{v}_{\mathbf{k}} = \frac{i\mathbf{k}}{k^2} \beta \delta_{\mathbf{k}}^r, \quad (11)$$

where  $\mathbf{v}_{\mathbf{k}}$  and  $\delta_{\mathbf{k}}^r$  are the Fourier coefficients of the velocity and real space density fields, respectively.

Here and throughout the paper we work in the ‘‘distant observer’’ limit, and assume that the observed region lies in the  $z$  direction (see e.g. Heavens & Taylor 1995, Zaroubi & Hoffman 1996 for the general case). Hence, we write  $\mu = \mathbf{k} \cdot \hat{\mathbf{z}}$ , and the Fourier transform of eq. (9) leads, for a given wavenumber  $\mathbf{k}$ ,

$$\delta_{\mathbf{k}}^s = \delta_{\mathbf{k}}^r (1 + \beta \mu^2). \quad (12)$$

The redshift space, dimensionless power spectrum  $\Delta_{3D}^s(\mathbf{k})$  is then

$$\Delta_{3D}^s(\mathbf{k}) = \Delta_{3D}^r(\mathbf{k}) (1 + \beta \mu^2)^2. \quad (13)$$

which is known as the Kaiser formula (Kaiser 1987). To avoid the proliferation of indices, we will hereafter drop indices when they characterise real space quantities.

### 3 LINEAR REDSHIFT DISTORTIONS IN 1D POWER SPECTRA

In this Section, we compute the 1D redshift space matter power spectrum in the linear regime. The bias factor is therefore  $b = 1$ . Moreover, since the strength of linear redshift distortions increases with  $\beta$ , we choose to present results at redshift  $z = 3$ . This choice is also aimed at facilitating the comparison between theory and observations (e.g. Croft *et al.* 1998, 2002; McDonald *et al.* 2000).

We aim at deriving an expression for the 1D power spectrum in redshift space,  $\Delta_{1D}^s$ , in terms of the 3D linear power spectrum in real space,  $\Delta_{3D}^r$ . To this extent we substitute  $\Delta_{3D}^s$  as given in terms of  $\Delta_{1D}^r$  in eq. (13) into the basic relation (6) and obtain

$$\Delta_{1D}^s(q) = q \int_q^\infty dk \frac{\Delta_{3D}^r(k)}{k^2} \left[ 1 + \beta \left( \frac{q}{k} \right)^2 \right]^2. \quad (14)$$

$\Delta_{3D}^r(k)$  is now the linear 3D power spectrum in real space. Eq. (14) is the counterpart of the Kaiser relation for 1D spectra. Defining the functions  $I_n(q)$  as

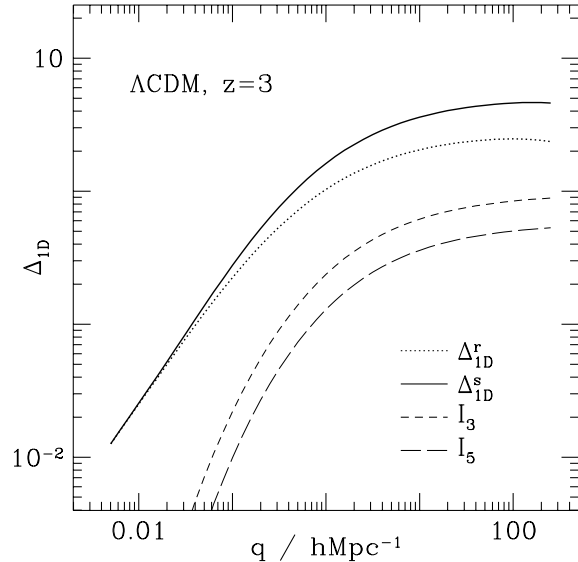


**Figure 1.** The real (dotted) and redshift space (solid) one-dimensional power spectra,  $\Delta_{1D}^r$  and  $\Delta_{1D}^s$ . The function  $I_3$  and  $I_5$  are also shown as short- and long-dashed curves respectively. The curves were computed at  $z = 3$  for a  $\Lambda$ CDM model of spectral index  $n_s = 1$ . On large scale, linear redshift distortions cancel out in the one-dimensional matter power spectra.

$$I_n(q) = q^n \int_q^\infty dk \frac{\Delta_{3D}^r}{k^{n+1}}, \quad (15)$$

we can write the 1D, redshift space power spectrum as follows,

$$\Delta_{1D}^s(q) = \Delta_{1D}^r(q) + 2\beta I_3(q) + \beta^2 I_5(q), \quad (16)$$

where we used the fact that  $I_1(q)$  is the 1D power spectrum in real space  $\Delta_{1D}^r$ . Using the relation (6), it is also possible to integrate the functions  $I_n$  by part and express  $\Delta_{1D}^s(q)$  as a function of  $\Delta_{1D}^r(q)$  alone.

#### 3.1 The linear PS in a $\Lambda$ CDM cosmology

In Fig 1, we show the real and redshift space 1D power spectra,  $\Delta_{1D}^r$  and  $\Delta_{1D}^s$ , as the dotted and solid curves respectively. They are computed using the 3D power spectrum given by the fitting formula of Bardeen *et al.* (1986) for a  $\Lambda$ CDM model. The cosmological parameters that we use are listed in Table 1. The  $\Lambda$ CDM model has a present-day, *rms* of fluctuations  $\sigma_8 = 0.9$  on scale  $8 h^{-1}\text{Mpc}$ , and a spectral index  $n_s$ . A value  $n_s = 0.9 - 1$  is consistent with the latest observations of the CMB, the large-scale structure and the Ly $\alpha$  forest, which constrain the spectral index to be  $n_s = 0.93 \pm 0.03$  on scale  $0.07 h\text{Mpc}^{-1}$  (Spergel *et al.* 2003).

##### 3.1.1 The large scale behaviour

In Fig. 1 we see that redshift distortions vanish on large scales, although one might have expected a large-scale effect

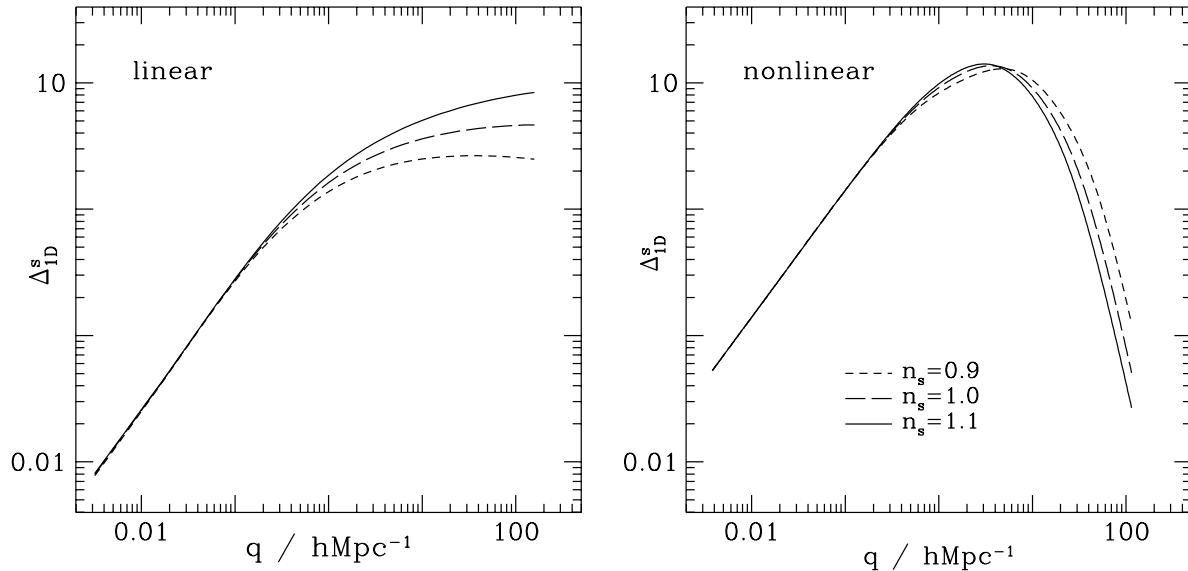


**Figure 2.** The linear (left panel) and nonlinear (right panel), 1D redshift space power spectra  $\Delta_{1D}^s$  for various spectral index :  $n_s = 0.9$  (short-dashed), 1 (long-dashed), and 1.1 (solid). In both panels, the curves corresponding to the power spectra with  $n_s \neq 1$  are shifted vertically to the  $n_s = 1$  curve on large scales. The results are for a  $\Lambda$ CDM model at  $z = 3$ .

**Table 1.** The main parameters of the CDM models considered in this paper.

	$\Omega_m$	$\Omega_\Lambda$	h
$\Lambda$ CDM	0.3	0.7	0.7
OCDM	0.3	0	0.7
SCDM	1	0	0.5

from the Kaiser formula. Moreover, the figure shows also that the slope of the redshift power spectrum approaches unity in the large-scale limit, irrespective of the spectral index. To explain this, let us examine in more detail the large scale behaviour of each of the terms on the r.h.s of (16). Consider first the term  $\Delta_{1D}^r$ . Using (6), we can express it in term of the 3D power spectrum  $\Delta_{3D}^r$  as

$$\frac{\Delta_{1D}^r}{q} = \int_q^\infty dk \frac{\Delta_{3D}^r(k)}{k^2}. \quad (17)$$

In CDM cosmological models  $\Delta_{3D}^r \sim k^{n_s+3}$  and  $k^{1-n_s}$  on large and small scales respectively. Thus, the integral in (17) converges as  $q$  tends to infinity so that  $\Delta_{1D}^r \sim q$  in that limit. Following similar arguments, we find  $I_3 \sim q^3$  and  $I_5 \sim q^{n_s+3}$  in that limit. Therefore, the main contribution to  $\Delta_{1D}^s$  on large scales is the term  $\Delta_{1D}^r \sim q$ .

### 3.1.2 The small scale behaviour

Fig. 1 shows that redshift distortions enhance the power by a factor of  $\sim 2$  on scales  $q \gtrsim 0.1 \text{ hMpc}^{-1}$ . On these scales  $\Delta_{1D}^s$  is very sensitive to the spectral index  $n_s$ . This is clear from

the left panel of Fig. 2, where the linear, 1D redshift space power spectrum is plotted for spectral index  $n_s = 0.9, 1$  and 1.1. Curves corresponding to models with  $n_s \neq 1$ , were shifted vertically so that they match the model  $n_s = 1$  on large scales. Since we are working in the linear regime, this matching can also be achieved by a change in  $\sigma_8$  for these models. For  $q \gtrsim 0.1 \text{ hMpc}^{-1}$ , the amplitude of the 1D, redshift space fluctuations increases significantly with the spectral index. Based on this, one would hope to constrain the spectral index from measurements on scale  $q \gtrsim 0.1 \text{ hMpc}^{-1}$ . However, as we will show next the small scale power spectrum in redshift space is strongly affected by nonlinear effects.

## 4 NONLINEAR REDSHIFT DISTORTIONS IN 1D POWER SPECTRA

So far we considered linear perturbations for which the 3D power spectra in redshift and real space are related by the Kaiser relation (13). At redshift  $z \sim 3$  however, nonlinear corrections are already important for wavenumbers  $|\mathbf{k}| \gtrsim 1 \text{ hMpc}^{-1}$ . As clearly seen from relation (6), nonlinearities contaminate  $\Delta_{1D}(q)$  at scales significantly larger than the nonlinear scale (e.g. Zaldarriaga & Scoccimarro & Hui 2003).

### 4.1 The nonlinear 3D power spectrum

Given the initial power spectrum we wish to estimate the non-linear 1D power spectrum in redshift space. Nonlinearities come in two different ways. First, the dynamical growth of density perturbations is faster than linear theory prediction on small scales. Second, nonlinear random and coher-

ent motions suppress the small-scale power in redshift space. This is because overdense regions with strong velocity shear are seen stretched along the LOS (the “finger of God” effect) in redshift space. This stretching wipes out the small-scale power in redshift space.

The nonlinear evolution of the 3D power spectrum in real space can be easily described by simple fitting formulae which have been calibrated using a large suite of N-body simulations (e.g. Hamilton *et al.* 1991; Jain *et al.* 1995; Peacock & Dodds 1996; Smith *et al.* 2003). We will use hereafter the fitting formula proposed in Smith *et al.* (2003) (cf. Appendix C of their paper) to model the nonlinear 3D power spectrum given an initial linear power spectrum.

Incorporating the effect of peculiar velocities is more complicated. The reason is the lack of a convenient relation, similar to the linear eq. (11), between the velocity and density in the nonlinear regime. However, several workers in the field have investigated the effect of peculiar motions on the 3D power spectrum in redshift space using N-body simulations (e.g. Peacock 1992; Peacock & Dodds 1994; Cole & Fisher & Weinberg 1995; Bromley, Warren & Zurek 1997; Magira, Jing & Suto 2000; Jing & Börner 2001). It was found that this effect can be modelled in the 3D power spectrum by multiplying the r.h.s. of eq. (13) with a filtering function of the form (Jing & Börner 2001),

$$D[k\mu\sigma_{12}] = \left[1 + \frac{1}{2}(k\mu\sigma_{12})^2 + \eta(k\mu\sigma_{12})^4\right]^{-1}. \quad (18)$$

where  $\sigma_{12}$  is the LOS pairwise velocity dispersion (PVD) of dark matter on scale  $k \sim 1/r$ , and  $\eta$  is a constant calibrated using numerical simulations. For illustration, we have  $\eta = 0.00759$  for a  $\Lambda$ CDM model. This scaling relation holds relatively well for  $k\mu\sigma_{12} \lesssim 20$ . The PVD of the dark matter,  $\sigma_{12}$ , can be computed directly from N-body simulation, but the calculation is rather tedious. Mo, Jing & Börner (1997) provide a simple, physically motivated fitting formula for  $\sigma_{12}(k)$ . This formula is a reasonable fit to the CDM cosmological models examined in the present paper. Note that at large separations, the pairwise velocity dispersion is  $\sigma_{12}(0) = \sqrt{2/3}\langle v_1^2 \rangle^{1/2}$ , where  $\langle v_1^2 \rangle^{1/2}$  is the density-weighted *rms* peculiar velocity of the dark matter. We also have typically  $\langle v_1^2 \rangle^{1/2} \approx 500 - 1000 \text{ km s}^{-1}$  in the CDM cosmological models considered here. Therefore, we can mimic the small-scale damping caused by nonlinear motions by combining the fitting formula (18) of Jing & Börner (2001) with the ansatz of Mo, Jing & Börner (1997). Although numerical simulations are needed to accurately calibrate  $D[k\mu\sigma_{12}]$  as a function of the cosmological model (in particular the spectral index  $n_s$ ) and redshift, we expect this approximation to be valid for  $n_s \approx 1$ .

## 4.2 The nonlinear 1D power spectrum

Following the previous discussion, we extend the validity of relation (14) to the nonlinear regime by computing the 1D power spectrum  $\Delta_{1D}^s$  from the 3D, redshift space power spectrum according to

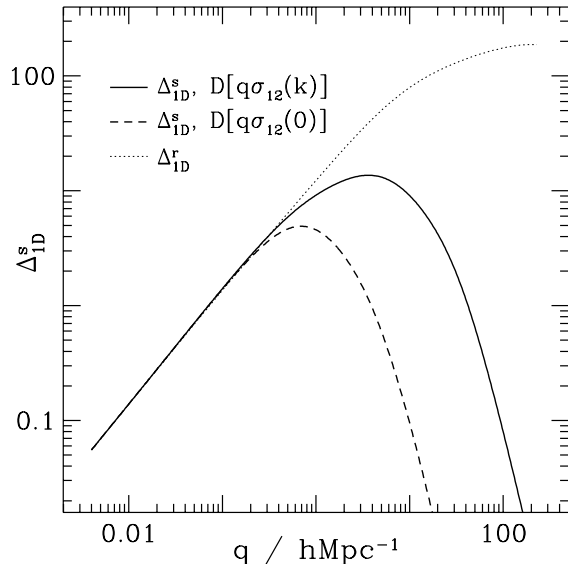


**Figure 3.** A comparison at  $z = 3$  between the nonlinear 1D, real and redshift space power spectra,  $\Delta_{1D}^r$  and  $\Delta_{1D}^s$ , for a  $\Lambda$ CDM model with  $n_s = 1$ . The dotted curve is  $\Delta_{1D}^r$ . The solid curve shows  $\Delta_{1D}^s$  with a damping factor  $D = D[q\sigma_{12}(k)]$ , whereas the dashed curve is  $\Delta_{1D}^s$  with  $D = D[q\sigma_{12}(0)]$ . The behaviour of  $\Delta_{1D}^s$  is very sensitive to the assumed filter  $D$ .

$$\Delta_{1D}^s(q) = q \int_q^\infty dk \frac{\Delta_{3D}^{NL}(k)}{k^2} \left[1 + \beta \left(\frac{q}{k}\right)^2\right]^2 D[q\sigma_{12}(k)]. \quad (19)$$

In the general case,  $\sigma_{12}$  is a function of  $k$  and the damping factor  $D[q\sigma_{12}(k)]$  cannot be extracted from the integral. In Fig. 3 we compare at  $z = 3$  the nonlinear 1D, real space power spectrum (dotted curve) with its redshift space counterpart as computed from eq. (19) (dotted curve). The damping factor  $D$  erases the power on scale  $q \gtrsim 1 \text{ hMpc}^{-1}$ . A comparison with the 1D power spectrum  $\Delta_{1D}^s$  as computed from a damping factor  $D = D[q\sigma_{12}(0)]$  (long-dashed) reveals also that  $\Delta_{1D}^s$  is very sensitive to the exact behaviour of  $\sigma_{12}(q)$ . Finally, it should be noted that, since the contribution from virialized dark matter haloes to the pairwise dispersion  $\sigma_{12}$  increases with time, the characteristic wavenumber of the cutoff decreases with decreasing redshift.

In this analysis, we did not take into account higher order terms of the Taylor expansion of the continuity equation (9) (see, for example, Cole, Fisher & Weinberg 1994 for a discussion of this effect). However, these corrections are implicitly included in the low-pass band filter  $D$ . One could also perform a perturbative calculation to address this issue in a more consistent way (e.g. Heavens, Matarrese & Verde 1998; Viel *et al.* 2004). Perturbation theory is useful for describing distortions in 3D power spectra in the mildly nonlinear regime. However, according to relation (6), 1D power spectra on a given scale are contaminated by the evolution of 3D power on all smaller scales, and one should therefore ensure that the 3D power spectrum decays rapidly enough on small scale before applying perturbation theory. In this paper we follow the practical approach outlined above.

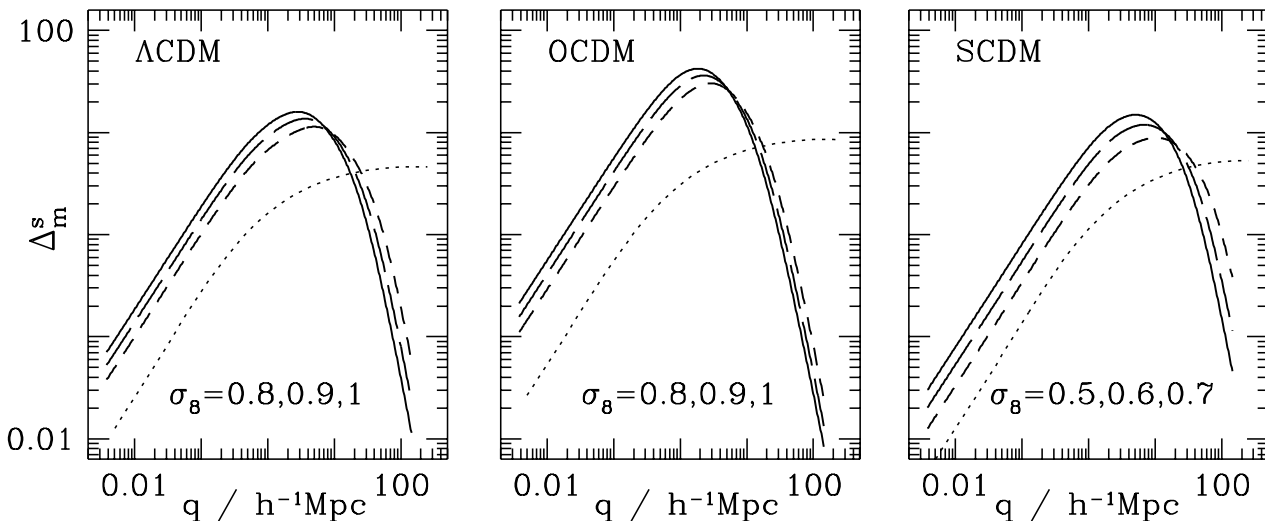


**Figure 4.** The nonlinear 1D, redshift space power spectrum  $\Delta_{1D}^s$  at  $z = 3$  for the CDM models of Table. 1, with spectral index  $n_s = 1$ . In each panel,  $\Delta_{1D}^s$  is plotted for three different  $\sigma_8$  as indicated on the Figure. The solid (short-dashed) curve corresponds to the highest (lowest) quoted values of  $\sigma_8$ . We also show as a dotted curve the linear  $\Delta_{1D}^s$  corresponding to the nonlinear  $\Delta_{1D}^s$  plotted as a long-dashed curve. For a given cosmological model, the amplitude of  $\Delta_{1D}^s$ , and the position of its maximum are sensitive to the value of  $\sigma_8$ .

### 4.3 Sensitivity to the cosmological parameters

#### 4.3.1 The large scale behaviour

To illustrate the dependence of the 1D power spectra on the cosmological parameters, we plot on Fig. 4 the nonlinear 1D, redshift space power spectrum  $\Delta_{1D}^s$ . It is computed from equations (14) and (19) for various CDM models :  $\Lambda$ CDM (left panel), OCDM (middle panel) and SCDM (right panel). The corresponding cosmological parameters are listed in Table 1. For each cosmological model, we plot  $\Delta_{1D}^s$  for three different values of  $\sigma_8$ , as quoted in Fig. 4. In each panel, the solid (short-dashed) shows  $\Delta_{1D}^s$  for the largest (lowest)  $\sigma_8$ . Note that the spectral index is set to  $n_s = 1$ . Fig. 4 illustrates the importance of nonlinear corrections, which drive the 1D redshift space power spectra  $\Delta_{1D}^s$  of various CDM models towards a power spectrum nearly insensitive to the cosmological parameters and primordial spectral index. This is a consequence of nonlinear gravitational dynamics, which drive the linear, 3D real space power spectrum  $\Delta_{3D}^s$  towards a universal power-law spectrum of effective spectral index  $n = 1.6$  (Scoccimarro & Frieman 1996, see also Zaldarriaga, Scoccimarro & Hui 2003). As a result, aliasing causes the effective spectral index  $n_{1D}$  to be insensitive to  $n_s$  on scale  $q \lesssim 1 \text{ hMpc}^{-1}$ . Fig. 4 demonstrates also that aliasing substantially enhances the large-scale normalisation of  $\Delta_{1D}^s$ . At redshift  $z = 3$ , the large-scale amplitude of the nonlinear power spectrum  $\Delta_{1D}^s$  is larger than its linear counterpart by a factor 5.6, 7.9 and 4.3 for the  $\Lambda$ , O and SCDM models respectively. Neglecting nonlinear corrections would therefore lead to a severe overestimation of  $\sigma_8$ .

#### 4.3.2 The small scale behaviour

As we can see from Fig. 4, the nonlinear 1D, redshift space power spectrum reaches its maximum for some  $q$  in the range  $1 - 10 \text{ hMpc}^{-1}$ . On smaller scale,  $\Delta_{1D}^s$  features a sharp cutoff due to nonlinear motions. The precise shape of the small-scale cutoff depends on the assumed filter  $D$ . It is sensitive to the amplitude of  $\sigma_{12}(q)$  which, for a given cosmological model, is mostly set by  $\sigma_8$ . As expected, the amplitude of the power spectrum decreases with  $\sigma_8$ , and  $\Delta_{1D}^s$  peaks at smaller scales. Therefore, although the nonlinear  $\Delta_{1D}^s$  does not seem to change much with  $\Omega_m$  and  $\Omega_\Lambda$ , its overall shape depends on the exact value  $\sigma_8$ . The right panel of Fig. 2 shows that the shape of the nonlinear  $\Delta_{1D}^s$  is also sensitive to the spectral index  $n_s$ . However, the small-scale nonlinear  $\Delta_{1D}^s$  is much less sensitive to  $n_s$  than that in the linear regime. There is obviously a degeneracy between  $\sigma_8$  and  $n_s$ . Unfortunately, since the fitting formulae of Mo, Jing & Börner (1997) and Jing & Börner (2001) were estimated for  $n_s = 1$  CDM numerical simulations, one has to extend the validity of these approximations to  $n_s \neq 1$  in order to address this issue any further.

## 5 DISCUSSION

In this paper we modelled in detail power spectra estimated from data given along lines of sight rather than in 3D space.

Redshift distortions on large scales, both in the linear and nonlinear regimes, vanish in power spectra estimated from data given along lines of sight. On small scales ( $q \gtrsim 1 \text{ hMpc}^{-1}$ ), linear redshift distortions enhance the power spectrum, but the nonlinear random motions and the

strong velocity shear work in the opposite direction of suppressing the power. The net result is that the nonlinear 1D power spectrum in redshift space falls below its counterpart in real space on small scales. On large scales however, they both have similar shapes, but the amplitude of the nonlinear power spectrum is significantly higher. The dimensionless 1D power spectrum peaks at a scale which depends on the pairwise velocity dispersion (PVD). The PVD is a strong function of the normalization of the power. Therefore the shape of  $\Delta_{1D}^s$  is set by  $\sigma_8$ , and to a lesser extent by the spectral index  $n_s$ . For the CDM models considered in this paper,  $\Delta_{1D}^s$  peaks at  $q \sim 1 - 10 \text{ hMpc}^{-1}$  which is roughly the scale at which the flux power spectrum  $\Delta_F$  of the Ly $\alpha$  forest peaks. Note that, on scale  $q \gtrsim 1 \text{ hMpc}^{-1}$ , the flux power spectrum is also sensitive to thermal broadening which is another redshift space effect (e.g. Theuns, Schaye & Haehnelt 2000). In a future work, we will model the Ly $\alpha$  flux power spectrum. We will also explore the implications of the observations on the cosmological model.

## 6 ACKNOWLEDGMENT

We would like to thank Saleem Zaroubi for useful discussions, and the anonymous referee for a careful reading of the manuscript. This Research was supported by the Binational Science Foundation, the German-Israeli Foundation for the Development of Science and Research, and the EC RTN network ‘‘Physics of the Intergalactic Medium’’.

## REFERENCES

- Abazajian K. and the SDSS team, 2003, *AJ*, 126, 2081  
 Ballinger W.E., Peacock J.A., Heavens A.F., 1996, *MNRAS*, 282, 877  
 Bardeen J.M., Bond J.R., Kaiser N., Szalay A.S., 1986, *ApJ*, 304, 15  
 Bromley B.C., Warren M.S., Zurek W.H., 1997, *ApJ*, 475, 414  
 Cole S., Fisher K.B., Weinberg D.H., 1994, *MNRAS*, 267, 785  
 Cole S., Fisher K.B., Weinberg D.H., 1995, *MNRAS*, 275, 51  
 Croft R.A.C., Weinberg D.H., Katz N., Hernquist L., 1998, *ApJ*, 495, 44  
 Croft R.A.C., Weinberg D.H., Pettini M., Hernquist L., Katz N., 1999, *ApJ*, 520, 1  
 Croft R.A.C., Weinberg D.H., Bolte M., Burles S., Hernquist L., Katz N., Kirkman D., Tytler D., 2002, *ApJ*, 581, 20  
 Desjacques V., Nusser A., in preparation  
 Fisher K.B., Scharf C.A., Lahav O., 1994, *MNRAS*, 266, 219  
 Fisher K.B., Nusser A., 1996, *MNRAS*, 279, L1  
 Hamilton A.J.S., Kumar P., Lu E., Matthews A., 1991, *ApJ*, 374, L1  
 Hamilton A.J.S., 1993, *ApJ*, 406, L47  
 Heavens A.F., Taylor A.N., 1995, *MNRAS*, 275, 483  
 Heavens A.F., Matarrese S., Verde L., 1998, *MNRAS*, 301, 797  
 Jain B., Mo H.J., White S.D.M., 1995, *MNRAS*, 276, L25  
 Jing Y.P., Börner G., 2001, *ApJ*, 547, 545  
 Kaiser N., 1987, *MNRAS*, 227, 1  
 Kaiser N., Peacock J.A., 1991, *ApJ*, 379, 482  
 Kang X., Jing Y.P., Mo H.J., Börner G., 2002, *MNRAS*, 336, 892  
 Lilje P.B., Efstathiou G., 1989, *MNRAS*, 236, 851  
 Loveday J., Efstathiou G., Maddox S.J., Peterson B.A., 1996, *ApJ*, 468, 1  
 Magira H., Jing Y.P., Suto Y., 2000, *ApJ*, 528, 30  
 McDonald P., Miralda-Escudé J., Rauch M., Sargent W.L.W., Barlow T.A., Cen R., Ostriker J.P., 2000, *ApJ*, 543, 1  
 McDonald P., 2003, *ApJ*, 585, 34  
 McGill C., 1990, *MNRAS*, 242, 428  
 Mo H.J., Jing Y.P., Börner G., 1997, *MNRAS*, 286, 979  
 Peebles P.J.E., 1980, *The Large Scale Structures of the Universe*, Princeton University Press  
 Peacock J.A., 1992, in Martinez V., Portilla M., Sáez D., eds, *New insights into the Universe*, Proc. Valencia summer school. Springer, Berlin, p.1  
 Peacock J.A., Dodds S.J., 1994, *MNRAS*, 267, 1020  
 Peacock J.A., Dodds S.J., 1996, *MNRAS*, 280, L19  
 Ratcliffe A., Shanks T., Broadbent A., Parker Q.A., Watson F.G., Oates A.P., Fong R., Collins C.A., 1996, *MNRAS*, 281, 47  
 Scoccimarro R., Frieman J.A., 1996, *ApJ*, 473, 620  
 Smith R.E., Peacock J.A., Jenkins A., White S.D.M., Frenk C.S., Pearce F.R., Thomas P.A., Efstathiou G., Couchman H.M.P., 2003, *MNRAS*, 341, 1311  
 Spergel D.N., Verde L., Peiris H.V., Komatsu E., Nolte M.R., and the WMAP team, 2003, *ApJS*, 148, 175  
 Taylor A.N., Hamilton A.J.S., *MNRAS*, 1996, 282, 767  
 Theuns T., Schaye J., Haehnelt M.G., 2000, *MNRAS*, 315, 600  
 Viel M., Matarrese S., Heavens A., Haehnelt M.G., Kim T.-S., Springel V., Hernquist L., 2004, *MNRAS*, 347, L26  
 Zaldarriaga M., Scoccimarro R., Hui L., 2003, *ApJ*, 590, 1  
 Zaroubi S., Hoffman Y., 1996, *ApJ*, 462, 25